Analytical Triangular Decoupling Internal Model Control of a Class of Two-Input, Two-Output (TITO) Systems with Delays

K. S. Ogunba[1], D. Fasiku[2], A. A. Fakunle[1] and O. Taiwo[2]

[1] Department of Electronic and Electrical Engineering, Obafemi Awolowo University, Ile-Ife, Nigeria.
[2] Process Systems Engineering Laboratory, Department of Chemical Engineering, Obafemi Awolowo University, Ile-Ife, Nigeria.

(Email Addresses: *kolaogunba@oauife.edu.ng, femtaiwo@yahoo.com,)*

Abstract: The Decoupling Internal Model Control (DIMC) technique is modified to achieve triangular decoupling for a class of two-input, two-output systems with delays. The closed-loop transfer function matrix that guarantees stability and triangular decoupling within the IMC framework is mathematically developed, and the corresponding centralized decoupling internal model controller calculated for systems with delays and right-half-plane zeros. The shifting of inverse responses and interactions is achieved to a single least-desired output so that for non-minimum-phase (NMP) two-input, two-output (TITO) systems with delays, one output has some delay but has no interacting behaviour or inverse response behaviour, while the less-desired output has substantial interaction and inverse response behaviour, with asymptotic tracking of setpoints for both outputs. A simulation example shows the effectiveness of the proposed method.

Keywords: Triangular Decoupling, Non-minimum-Phase Systems, Decoupling Internal Model Control, Multivariable Control, Two-Input, Two-Output Systems, Moment Matching.

1. Introduction

Internal Model Control (IMC) for open-loop-stable single-input, single-output (SISO) systems provides attractive features of design simplicity, guarantees of closed-loop stabilty and zero steady-state offset, theoretical possibility of perfect control and a transparent technique of robust control (Garcia and Morari, 1982). Extensions of linear SISO IMC have been actualized to a wide range of systems (Morari and Zafiriou, 1989). Extensions to linear, square, open-loop-stable multivariable systems have been substantially explored (Garcia and Morari, 1985; Holt and Morari, 1985).

For control of open-loop-stable systems, the extension of linear SISO IMC to linear, square, minimum-phase delay-free, multivariable systems is trivial, requiring simple transfer-function-matrix inversion and diagonal filter-matrix augmentation. The extension to linear, square, non-minimum-phase delay-free, multivariable systems is however non-trivial, because of the presence of RHP transmission zeros and the infinitely-many possible matrix factorization techniques. The consideration of optimality in factorization of matrices for multivariable IMC leads to the complicated solution of Frank (1974), while the limiting cases are the factorization procedure achieving dynamic decoupling, on one hand, and triangular decoupling, on the other (Holt and Morari, 1985). The Inner-Outer Factorization technique achieves more closeness to optimality than the decoupling techniques and has been successfully applied to multivariable delay-free IMC of systems, although it involves a lengthier design process that involves the conversion to state space and the solution to an Algebraic Riccati Equation (Morari and Zafiriou, 1989).

The triangular decoupling control problem has been solved using a variety of techniques over the past five decades. The existence of RHP zeros imposes bandwidth limitations on all channels in dynamic decoupling and the option of restricting these limitations to a single, least-desired channel is an attractive alternative, with the relaxing of the decoupling objective on the least desired output (Goodwin *et al.*, 2000). Several authors have provided solutions to the triangular decoupling problem in different ways and for different systems (Morse and Wonham, 1970; Descusse and Lizarzaburu, 1979; Nijmeijer, 1984; Koumboulis and Skarpetis, 2000; Wang, 2007; Koumboulis and Panagiotakis, 2008; Nguyen and Su, 2009; Shen and Wei, 2015; Li, Jia and Liu, 2017; Koumboulis and Kouvakas, 2018).

The extension of the aforementioned multivariable IMC designs to linear, square, open-loop-stable, multivariable systems with delays is appealing but has not been directly possible because of the irrationality of the inverse of a transfer function matrix with delays. Over the last two decades, the use of dynamic decoupling concepts has made IMC implementations possible for multivariable systems with delays (Wang *et al.*, 2002; Liu *et al.*, 2006; Garrido *et al.*, 2014). However, the use of the triangular decoupling concept to achieve controller design for delayed systems using the IMC concept has not been explored in literature. In this study, the decoupling IMC configuration is used to develop centralized triangular decoupling controllers for linear, square, open-loop-stable multivariable systems. The triangular closed-loop transfer function matrix that guarantees triangular decoupling for a system with a single RHP transmission zero is derived and the centralized multivariable IMC controller achieving it is calculated and approximated using appropriate model-reduction techniques. A simulation example using the Quadruple-Tank Process with Dead Times will show the effectiveness of the designs.

2. Assumptions for Analytical Triangular Decoupling IMC

The centralized MIMO IMC for a 2 x 2 multivariable system is shown in Figure 1.

The output transform $\boldsymbol{Y(s)}$ is related to the input transform $\boldsymbol{R(s)}$ by

$$\boldsymbol{Y(s) = GC\left(I + [G - \hat{G}]C\right)^{-1}R + \{I - \hat{G}C\}\left(I + [G - \hat{G}]C\right)^{-1}D} \quad (1)$$

where $\boldsymbol{D, \hat{G}, C, R}$ and $\boldsymbol{G}$ respectively represent the Laplace transforms of the output disturbance vector, model of plant, centralized internal model controller, command signal vector and plant transfer function, and $\boldsymbol{I}$ is the $\mathbf{2 \times 2}$ identity matrix.

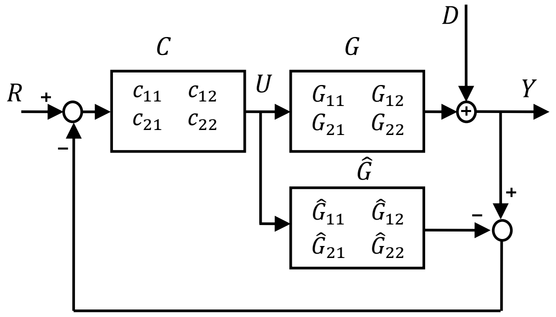

Figure 1: Centralized Internal Model Control Structure for TITO Systems

With the assumption of the absence of output disturbance, the closed-loop transfer function matrix $\boldsymbol{H(s)}$ becomes

$$\boldsymbol{H(s) = GC\left(I + [G - \hat{G}]C\right)^{-1}} \quad (2)$$

With the assumption of perfect model-process match, the system becomes effectively open-loop, with the closed-loop transfer function matrix becoming

$$\boldsymbol{H(s) = G(s)C(s)} \quad (3)$$

In addition to the aforementioned assumptions, the assumptions of non-singularity of the matrices $\boldsymbol{G(s)}$ and $\boldsymbol{C(s)}$ at $s = 0$ and the absence of coupling in the tuning of the columns of the controller matrix $\boldsymbol{C(s)}$ are made according to the preconditions specified by Liu and co-workers (2006).

3. Development of Desired Triangular Closed-Loop Transfer Function Matrix

If the plant and controller transfer function matrices of rational elements plus delays are respectively given by

$$\boldsymbol{G(s) = \begin{bmatrix} G_{11}(s) & G_{12}(s) \\ G_{21}(s) & G_{22}(s) \end{bmatrix}} \quad (4)$$

$$\boldsymbol{C(s) = \begin{bmatrix} C_{11}(s) & C_{12}(s) \\ C_{21}(s) & C_{22}(s) \end{bmatrix}} \quad (5),$$

where

$$\boldsymbol{G_{ij}(s) = G_{ijr}e^{-\theta_{gij}s}; i = 1,2; j = 1,2; \theta_{gij} \geq 0} \quad (6)$$

$$\boldsymbol{C_{ij}(s) = C_{ijr}e^{-\theta_{cij}s}; i = 1,2; j = 1,2; \theta_{cij} \geq 0} \quad (7)$$

(with $\boldsymbol{G_{ijr}}$ and $\boldsymbol{C_{ijr}}$ being rational open-loop-stable transfer functions), then for plant inputs being $\boldsymbol{u_1, u_2}$ and plant outputs being $\boldsymbol{y_1, y_2}$, triangular decoupling is achieved such that interactions and inverse responses are shifted to $\boldsymbol{y_2}$, with output $\boldsymbol{y_1}$ being non-interacting and without inverse response behaviour, the desired closed-loop transfer function matrix $\boldsymbol{H(s)}$, with the assumption of the presence of a single RHP transmission zero at $\boldsymbol{s = z}$ for the system, can be obtained using a modification of the technique of Holt and Morari (1985) to yield the matrix of eqn. (8) i.e.

$$\boldsymbol{H = \begin{bmatrix} H_{11} & 0 \\ H_{21} & H_{22} \end{bmatrix} = \begin{bmatrix} \frac{e^{-\theta_1 s}}{\tau_1 s+1} & 0 \\ \frac{z\beta_1 s}{s+z} \cdot \frac{e^{-\theta_1 s}}{\tau_1 s+1} & \frac{e^{-\theta_2 s}}{\tau_2 s+1}\left(\frac{-s+z}{s+z}\right) \end{bmatrix}} \quad (8),$$

where $\boldsymbol{\beta_1}$ is a constant to be determined.

The centralized controller becomes

$$\boldsymbol{C(s) = G^{-1}(s)H(s)} \quad (9)$$

and if the inverse of the transfer function matrix of the plant is given by

$$\boldsymbol{G^{-1}(s) = \frac{P(s)}{(-s+z)M(s)}\begin{bmatrix} \hat{g}_{11}(s) & \hat{g}_{12}(s) \\ \hat{g}_{21}(s) & \hat{g}_{22}(s) \end{bmatrix}} \quad (10),$$

where $\boldsymbol{P(s)}$ is the pole polynomial of the system, $\boldsymbol{(-s+z)M(s)}$ is the zero polynomial of the system, with $\boldsymbol{M(s)}$ having only negative roots, and $\boldsymbol{\hat{g}_{ij}}$ is the $\boldsymbol{(i,j)}$th element of the adjoint of the plant's transfer function matrix, then the centralized controller $\boldsymbol{C(s)}$ becomes

$$\boldsymbol{C = \frac{P(s)}{(-s+z)M(s)}\begin{bmatrix} \left(\hat{g}_{11} + \hat{g}_{12}\frac{z\beta_1 s}{s+z}\right)\frac{e^{-\theta_1 s}}{\tau_1 s+1} & \hat{g}_{12}\left(\frac{-s+z}{s+z}\right)\frac{e^{-\theta_2 s}}{\tau_2 s+1} \\ \left(\hat{g}_{21} + \hat{g}_{22}\frac{z\beta_1 s}{s+z}\right)\cdot\frac{e^{-\theta_1 s}}{\tau_1 s+1} & \hat{g}_{22}\left(\frac{-s+z}{s+z}\right)\frac{e^{-\theta_2 s}}{\tau_2 s+1} \end{bmatrix}} \quad (11)$$

Equation 11 will only be stable only if each of $\boldsymbol{\left(\hat{g}_{i1} + \hat{g}_{i2}\frac{z\beta_1 s}{s+z}\right)}$, $\boldsymbol{i = 1, 2}$, has the expression $\boldsymbol{(-s+z)}$ as one of its factors.

Theorem: For an open-loop-stable two-input, two-output system with delays and with a single RHP transmission zero at $s = z$, the expression

$$\boldsymbol{v_i = \hat{g}_{i1} + \hat{g}_{i2}\frac{z\beta_1 s}{s+z}, i = 1,2} \quad (12)$$

has the expression $\boldsymbol{(-s+z)}$ as one of its factors if and only if

$$\boldsymbol{\beta_1 = -\frac{2\hat{g}_{j1}(z)}{z\hat{g}_{j2}(z)}} \quad (13)$$

for an arbitrary $\boldsymbol{j}$.

Proof:

For $\boldsymbol{\beta_1}$ to make $\boldsymbol{v_i}$ to have a factor $\boldsymbol{(-s+z)}$, then

$$\boldsymbol{v_i|_{s=z} = \left[\hat{g}_{i1} + \hat{g}_{i2}\frac{z\beta_1 s}{s+z}\right]|_{s=z} = 0} \quad (14),$$

meaning that

$$\boldsymbol{[\hat{g}_{i1}(s+z) + \hat{g}_{i2}z\beta_1 s]|_{s=z} = 0} \quad (15)$$

or

$$\boldsymbol{2z\hat{g}_{i1} + z^2\hat{g}_{i2}\beta_1 = 0} \quad (16)$$

leading to

$$\boldsymbol{\beta_1 = -\frac{2z\hat{g}_{j1}(z)}{z^2\hat{g}_{j2}(z)} = -\frac{2\hat{g}_{j1}(z)}{z\hat{g}_{j2}(z)}} \quad (17)$$

Using the Theorem in eqn. (11), the Centralized IMC Controller achieving Triangular Decoupling is therefore

$$\boldsymbol{C} = \frac{P(s)}{(-s+z)M(s)} \begin{bmatrix} \left((-s+z)M_2(s)\right)\frac{e^{-\theta_1 s}}{\tau_1 s+1} & -G_{12}\left(\frac{-s+z}{s+z}\right)\frac{e^{-\theta_2 s}}{\tau_2 s+1} \\ (-s+z)M_3(s).\frac{e^{-\theta_1 s}}{\tau_1 s+1} & G_{11}\left(\frac{-s+z}{s+z}\right)\frac{e^{-\theta_2 s}}{\tau_2 s+1} \end{bmatrix} \quad \textbf{(18)}$$

where $\boldsymbol{M}$, $\boldsymbol{M_2}$ and $\boldsymbol{M_3}$ are expressions without RHP roots, leading to centralized Analytical Triangular Decoupling IMC controller achieving "perfect y_1 with delay" as

$$\begin{bmatrix} C_{11} & C_{12} \\ C_{21} & C_{22} \end{bmatrix} = \begin{bmatrix} \frac{P(s)M_2(s)e^{-\theta_1 s}}{M(s)(\tau_1 s+1)} & \frac{-P(s)G_{12}(s)e^{-\theta_2 s}}{(s+z)(\tau_2 s+1)M(s)} \\ \frac{P(s)M_3(s)e^{-\theta_1 s}}{M(s)(\tau_1 s+1)} & \frac{P(s)G_{11}(s)e^{-\theta_2 s}}{(s+z)(\tau_2 s+1)M(s)} \end{bmatrix} \quad \textbf{(19)}$$

Similarly, if the "non-interacting, minimum-phase output with delay" is y_2 i.e. the less-desired output is y_1, then eqn. (3) becomes

$$\boldsymbol{GC} = \begin{bmatrix} H_{11} & H_{12} \\ 0 & H_{22} \end{bmatrix} = \begin{bmatrix} \left(\frac{-s+z}{s+z}\right)\left(\frac{e^{-\theta_1 s}}{\tau_1 s+1}\right) & \frac{z\beta_{re,2}s}{s+z}.\frac{e^{-\theta_2 s}}{\tau_2 s+1} \\ 0 & \frac{e^{-\theta_2 s}}{\tau_2 s+1} \end{bmatrix} \quad \textbf{(20)}$$

where $\boldsymbol{\beta_{re,2}}$ is to be determined.

If we define the rearranged transfer function matrix of plant as

$$\boldsymbol{G_{rearr}} = \begin{bmatrix} G_{22} & G_{21} \\ G_{12} & G_{11} \end{bmatrix} \quad \textbf{(21)}$$

and the adjoint of the matrix as

$$\boldsymbol{adj(G_{rearr})} = \begin{bmatrix} \hat{g}_{re,11} & \hat{g}_{re,12} \\ \hat{g}_{re,21} & \hat{g}_{re,22} \end{bmatrix} = \begin{bmatrix} G_{11} & -G_{21} \\ -G_{12} & G_{22} \end{bmatrix} \quad \textbf{(22)},$$

then, the closed-loop transfer function matrix becomes lower-triangular as in eqn. (8) and repetition of the procedure that led to eqn. (19) yields the centralized Analytical Triangular Decoupling IMC controller achieving "perfect y_2 with delay" of eqn. (23):

$$\begin{bmatrix} C_{11} & C_{12} \\ C_{21} & C_{22} \end{bmatrix} = \begin{bmatrix} \frac{P(s)G_{22}(s)e^{-\theta_1 s}}{(s+z)(\tau_1 s+1)M(s)} & \frac{P(s)M_4(s)e^{-\theta_2 s}}{(\tau_2 s+1)M(s)} \\ \frac{-P(s)G_{21}(s)e^{-\theta_1 s}}{(s+z)(\tau_1 s+1)M(s)} & \frac{P(s)M_5(s)e^{-\theta_2 s}}{(\tau_2 s+1)M(s)} \end{bmatrix} \quad \textbf{(23)}$$

where $\boldsymbol{M_4}$ and $\boldsymbol{M_5}$ are expressions without RHP roots, and $\boldsymbol{P(s)}$ and $\boldsymbol{M(s)}$ are as defined for eqn. (18).

4. Generalized Analytical Triangular DIMC for Square MIMO NMP Systems with Delays

For an $\boldsymbol{n}$ **x** $\boldsymbol{n}$ open-loop-stable system $\boldsymbol{G(s)}$ with delays and a single RHP zero at $\boldsymbol{s = z}$, represented by the transfer function matrix

$$\boldsymbol{G(s)} = \begin{bmatrix} G_{11}(s) & \dots & G_{1n}(s) \\ \vdots & \ddots & \vdots \\ G_{n1}(s) & \dots & G_{nn}(s) \end{bmatrix}, \quad \textbf{(24)},$$

it can be shown that the $\boldsymbol{n}$ **x** $\boldsymbol{n}$, analytically-derived triangularly decoupling internal model controller that shifts the inverse response behaviour and control-loop interactions to the least desired output $\boldsymbol{y_n}$ is given by

$$\boldsymbol{C(s)} = \begin{bmatrix} C_{11}(s) & \dots & C_{1n}(s) \\ \vdots & \ddots & \vdots \\ C_{n1}(s) & \dots & C_{nn}(s) \end{bmatrix} =$$

$$\begin{bmatrix} \frac{P(s)M_{11}(s)e^{-\theta_1 s}}{M(s)(\tau_1 s+1)} & \dots & \frac{P(s)M_{1,n-1}(s)e^{-\theta_{n-1} s}}{M(s)(\tau_{n-1} s+1)} & \frac{P(s)\hat{g}_{1n}(s)e^{-\theta_n s}}{(s+z)(\tau_n s+1)M(s)} \\ \vdots & \ddots & \vdots & \vdots \\ \frac{P(s)M_{n1}(s)e^{-\theta_1 s}}{M(s)(\tau_1 s+1)} & \dots & \frac{P(s)M_{n,n-1}(s)e^{-\theta_{n-1} s}}{M(s)(\tau_{n-1} s+1)} & \frac{P(s)\hat{g}_{nn}(s)e^{-\theta_n s}}{(s+z)(\tau_n s+1)M(s)} \end{bmatrix} \quad \textbf{(25)}$$

where $\boldsymbol{P(s)}$, $\boldsymbol{M(s)}$ and $\boldsymbol{\hat{g}_{ij}}$ are as defined in eqn. (10), $\boldsymbol{M_{ij}}$ $(\boldsymbol{j = 1, \dots, n-1; j = 1, \dots, n-1})$ is the $\boldsymbol{(i,j)}$th expression without RHP roots determined after the calculation of $\boldsymbol{\beta_i}$ $(\boldsymbol{i = 1, \dots, n-1})$, the constant that ensures the presence of the term $\boldsymbol{(-s+z)}$ as a factor of $\left(\boldsymbol{\hat{g}_{ij} + \hat{g}_{in}\frac{z\beta_j s}{s+z}}\right)$, $\boldsymbol{i = 1, \dots, n-1; j = 1, \dots, n-1}$, and $\boldsymbol{\theta_i}$ and $\boldsymbol{\tau_i}$ $(\boldsymbol{i = 1, \dots, n})$ are the closed-loop time delay and tuning parameter respectively. Due to space economy, the details will be presented in subsequent publications.

5. Approximation of Plant Transfer Function Matrix Determinants

In the paper by Liu and co-workers (2006), the procedure for calculating the dynamic decoupling internal model controller involved representing a TITO system by the transfer function matrix of first-order-plus-delay elements:

$$\boldsymbol{G(s)} = \begin{bmatrix} \frac{K_{11}e^{-\theta_{11}s}}{\tau_{11}s+1} & \frac{K_{12}e^{-\theta_{12}s}}{\tau_{12}s+1} \\ \frac{K_{21}e^{-\theta_{21}s}}{\tau_{21}s+1} & \frac{K_{22}e^{-\theta_{22}s}}{\tau_{22}s+1} \end{bmatrix} \quad \textbf{(26)}$$

and the calculation of the controller $\boldsymbol{C(s)}$ as

$$\boldsymbol{C(s)} = \frac{1}{1-G^0 e^{-\Delta\theta.s}} * \begin{bmatrix} \frac{(\tau_{11}s+1)e^{\theta_{11}s}H_1}{K_{11}} & \frac{-K_{12}(\tau_{11}s+1)(\tau_{22}s+1)e^{(\theta_{11}+\theta_{22}-\theta_{12})s}}{K_{11}K_{22}(\tau_{12}s+1)} \\ \frac{-K_{21}(\tau_{11}s+1)(\tau_{22}s+1)e^{(\theta_{11}+\theta_{22}-\theta_{21})s}}{K_{11}K_{22}(\tau_{21}s+1)} & \frac{(\tau_{22}s+1)e^{\theta_{22}s}H_2}{K_{22}} \end{bmatrix} \quad \textbf{(27)}$$

where

$$\boldsymbol{F(s)} = \frac{1}{1-G^0 e^{-\Delta\theta.s}} \quad \textbf{(28)}$$

$$\boldsymbol{G^0(s)} = \frac{K_{12}K_{21}(\tau_{11}s+1)(\tau_{22}s+1)}{K_{11}K_{22}(\tau_{12}s+1)(\tau_{21}s+1)} \quad \textbf{(29)}$$

$$\boldsymbol{\Delta\theta} = |\theta_{11} + \theta_{22} - \theta_{12} - \theta_{21}| \quad \textbf{(30)}$$

$$\boldsymbol{H_i(s)} = \frac{1}{\tau_i s+1} e^{-\theta_i s} \prod_{j=1}^{v} \frac{-s+z_j}{s+z_j} \; (\boldsymbol{i = 1, 2}) \quad \textbf{(31)}$$

The expression $\boldsymbol{F(s)}$ in eqn. (28) was then approximated using moment matching and then multiplied into the matrix expression of eqn. (27), with the tuning parameters $\boldsymbol{\tau_i}$ $(\boldsymbol{i = 1, 2})$ characteristic of IMC implementations retained in the computations.

The procedure above is modified into the Analytical Triangular Decoupling IMC procedure without reduction of any of the elements of the original transfer function matrix. The terms $\boldsymbol{F}$, $\boldsymbol{G^0}$ and $\boldsymbol{\Delta\theta}$ are determined according to eqns. (28), (29) and (30) respectively, while eqn. (31) is replaced with eqn. (8) (perfect $\boldsymbol{y_1}$ with delays) and eqn. (20) (perfect $\boldsymbol{y_2}$ with delays).

6. Robustness Analysis of Designed Control Systems

For the robustness analysis of the closed-loop systems using the designed controllers, μ-analysis was performed. The uncertainty weight was represented as a diagonal multiplicative input uncertainty.

$$\boldsymbol{W_I} = \textbf{diag}\,(\boldsymbol{w_i, w_i});\; \boldsymbol{w_i} = \frac{s+0.2}{0.5s+1} \quad \textbf{(32)}$$

The chosen uncertainty weight indicates an uncertainty of **20%** in the process inputs, in the low frequency range, and an uncertainty of **200%** in the process inputs, in the high frequency range; attaining **100%** uncertainty at **1 rad/sec**.

The performance weight was also chosen to be:

$$\boldsymbol{W_P} = \boldsymbol{diag}\ (\boldsymbol{w_p}, \boldsymbol{w_p}); \quad \boldsymbol{w_p} = \frac{\frac{s}{2.3}+0.002}{s} \qquad (33)$$

This weight specifies an integral action (zero steady state error), peak sensitivity, $\boldsymbol{Ms}$=**2.3** (with an implication that Gain Margin $\boldsymbol{GM} \geq \boldsymbol{1.77}$ and Phase Margin $\boldsymbol{PM} \geq \boldsymbol{25.110}$), and bandwidth frequency=**0.002 rad/sec**. The structured singular value of robust stability (μ_{RS}), and robust performance (μ_{RP}) must be less than unity (Skogestad and Postlethwaite, 2005), as expressed below:

$$\mu_{RS} = \mu[-\boldsymbol{W_I}(\boldsymbol{s})\boldsymbol{T_I}(\boldsymbol{s})] < \boldsymbol{1} \quad \forall\omega \qquad (34)$$

$$\mu_{RP} = \mu\begin{bmatrix} -\boldsymbol{W_I}(\boldsymbol{s})\boldsymbol{T_I}(\boldsymbol{s}) & -\boldsymbol{W_I}(\boldsymbol{s})\boldsymbol{K}(\boldsymbol{s})\boldsymbol{S}(\boldsymbol{s}) \\ \boldsymbol{W_P}(\boldsymbol{s})\boldsymbol{S}(\boldsymbol{s})\boldsymbol{G}(\boldsymbol{s}) & \boldsymbol{W_P}(\boldsymbol{s})\boldsymbol{S}(\boldsymbol{s}) \end{bmatrix} < \boldsymbol{1} \ \forall\omega \qquad (35)$$

where μ is the structured singular value, $\boldsymbol{K}$ is the centralized feedback controller, $\boldsymbol{S}(\boldsymbol{s})$ and $\boldsymbol{T_I}(\boldsymbol{s})$ are the sensitivity function and complementary sensitivity function respectively.

Because of the conventional feedback form with which the uncertainties were formulated, each controller $\boldsymbol{C}(\boldsymbol{s})$ in the IMC configuration was converted to the equivalent conventional feedback controller $\boldsymbol{K}(\boldsymbol{s})$ using the formula.

$$\boldsymbol{K}(\boldsymbol{s}) = \boldsymbol{C}(\boldsymbol{s})[\boldsymbol{I} - \boldsymbol{G}(\boldsymbol{s})\boldsymbol{C}(\boldsymbol{s})]^{-1} \qquad (36)$$

7. Simulation Example: NMP Quadruple-Tank Process with Dead Times

The transfer function matrix of the **non-minimum-phase** configuration of the Quadruple-Tank Process with Dead Times (QTPwDTs) was presented by Shneidermann and Palmor (2010) as

$$\boldsymbol{G}(\boldsymbol{s}) = \begin{bmatrix} \frac{0.834}{6.57s+1}e^{-5s} & \frac{1.39}{(10.231s+1)(6.57s+1)}e^{-7s} \\ \frac{1.271}{(14.05s+1)(11.29s+1)}e^{-9s} & \frac{0.757}{11.29s+1}e^{-6s} \end{bmatrix} \qquad (37)$$

The system has an RHP transmission zero at **0.0419**.

For shifting of inverse response behaviour to $\boldsymbol{y_2}$, $\boldsymbol{\beta_1}$ was determined to be 33.5288 and $\boldsymbol{F}(\boldsymbol{s})$, written as $\boldsymbol{F_{uy1}}(\boldsymbol{s})$ in eqn. (38), was calculated to be

$$\boldsymbol{F_{uy1}}(\boldsymbol{s}) = \frac{-s+0.0418558}{\left(1 - \frac{2.79613\, e^{-5\,s}}{(10.231\,s+1)(14.05\,s+1)}\right)} \qquad (38)$$

and this was approximated using moment matching to $\boldsymbol{F_{app1}}$, where

$$\boldsymbol{F_{app1}}(\boldsymbol{s}) = \frac{-\,3.36694\,s^2 - 0.566899\,s - 0.0233034}{1.0318\,s^2 + 2.6351\,s + 1} \qquad (39)$$

After appropriate substitutions, the eventual controller achieving shifting of inverse response behaviour and interactions to $\boldsymbol{y_2}$ calculated as

$$\boldsymbol{C_{unr\_perfy1}}(\boldsymbol{s}) = \begin{bmatrix} \boldsymbol{C_{uy1-11}}(\boldsymbol{s}) & \boldsymbol{C_{uy1-12}}(\boldsymbol{s}) \\ \boldsymbol{C_{uy1-21}}(\boldsymbol{s}) & \boldsymbol{C_{uy1-22}}(\boldsymbol{s}) \end{bmatrix} \qquad (40)$$

where

$$\boldsymbol{C_{uy1-11}}(\boldsymbol{s}) = \frac{\left(\begin{matrix} -\,0.166s^6 - 0.555\,s^5 - 0.604s^4 - 0.192\,s^3 \\ -\,0.026\,s^2 - 0.001599\,s - 0.000037 \end{matrix}\right)e^{-3.13s}}{\left(\begin{matrix} 1.03s^6 + 3.03\,s^5 + 2.055s^4 + 0.518s^3 \\ +\,0.059\,s^2 + 0.003s + 0.000055 \end{matrix}\right)(\tau_1 s+1)} \qquad (41)$$

$$\boldsymbol{C_{uy1-12}}(\boldsymbol{s}) = \frac{(\,83.692s^3 + 21.504\,s^2 + 1.83\,s + 0.051\,)e^{-7\,s}}{(\,10.56\,s^4 + 28.43\,s^3 + 14.04\,s^2 + 1.54\,s + 0.042)(\tau_2 s+1)} \qquad (42)$$

$$\boldsymbol{C_{uy1-21}}(\boldsymbol{s}) = \frac{\left(\begin{matrix} 36.29\,s^6 + 29.6\,s^5 + 8.73\,s^4 + 1.24\,s^3 + 0.091\,s^2 \\ +\,0.0033\,s + 0.000045 \end{matrix}\right)e^{-2.093\,s}}{\left(\begin{matrix} 1.03s^6 + 3\,s^5 + + 1.977s^4 + 0.471s^3 + 0.05s^2 \\ +\,0.00235s + 0.00004 \end{matrix}\right)(\tau_1 s+1)} \qquad (43)$$

$$\boldsymbol{C_{uy1-22}}(\boldsymbol{s}) = \frac{(-\,50.2151\,s^3 - 12.9025\,s^2 - 1.09643\,s - 0.030784)e^{-5\,s}}{(\,1.0318\,s^3 + 2.67829\,s^2 + 1.11029\,s + 0.041856\,)(\tau_2 s+1)} \qquad (44)$$

For shifting of inverse response behaviour to $\boldsymbol{y_1}$, $\boldsymbol{\beta_{re,2}}$ was determined to be 67.9539 and $\boldsymbol{F}(\boldsymbol{s})$, written as $\boldsymbol{F_{uy2}}(\boldsymbol{s})$ in eqn. (45), was calculated to be

$$\boldsymbol{F_{uy2}}(\boldsymbol{s}) = \frac{-s+0.0418558}{\left(1 - \frac{2.79613\, e^{-5\,s}}{(10.231\,s+1)(14.05\,s+1)}\right)} \qquad (45)$$

and this was approximated using moment matching to $\boldsymbol{F_{app2}}$, where

$$\boldsymbol{F_{app2}} = \frac{-\,3.36694\,s^2 - 0.566899\,s - 0.0233034}{1.0318\,s^2 + 2.6351\,s + 1} \qquad (46)$$

After appropriate substitutions, the eventual controller achieving shifting of inverse response behaviour and interactions to $\boldsymbol{y_1}$ calculated as

$$\boldsymbol{C_{unr\_perfy2}}(\boldsymbol{s}) = \begin{bmatrix} \boldsymbol{C_{uy2-11}}(\boldsymbol{s}) & \boldsymbol{C_{uy2-12}}(\boldsymbol{s}) \\ \boldsymbol{C_{uy2-21}}(\boldsymbol{s}) & \boldsymbol{C_{uy2-22}}(\boldsymbol{s}) \end{bmatrix} \qquad (47)$$

where

$$\boldsymbol{C_{uy2-11}}(\boldsymbol{s}) = \frac{(-\,26.52\,s^3 - 8.503s^2 - 0.863s - 0.028)e^{-5\,s}}{(1.0318\,s^3 + 2.67829\,s^2 + 1.11029\,s + 0.0418558)(\tau_1 s+1)} \qquad (48)$$

$$\boldsymbol{C_{uy2-12}}(\boldsymbol{s}) = \frac{\left(\begin{matrix} 19.0105\,s^6 + 22.78\,s^5 + 8.02\,s^4 + 1.2855\,s^3 + 0.105\,s^2 \\ +\,0.00425s + 0.000068 \end{matrix}\right)e^{-2.83s}}{\left(\begin{matrix} 1.0318\,s^6 + 3.02758\,s^5 + 2.055s^4 + 0.518s^3 + 0.0588s^2 \\ +\,0.003s + 0.000055 \end{matrix}\right)(\tau_2 s+1)} \qquad (49)$$

$$\boldsymbol{C_{uy2-21}}(\boldsymbol{s}) = \frac{(44.4983\,s^3 + 14.2652\,s^2 + 1.44836\,s + 0.0468771\,)e^{-8\,s}}{(14.4967\,s^4 + 38.6618\,s^3 + 18.2779\,s^2 + 1.69837\,s + 0.0418558)(\tau_1 s+1)} \qquad (50)$$

$$\boldsymbol{C_{uy2-22}}(\boldsymbol{s}) = \frac{\left(\begin{matrix} -\,0.192103\,s^6 - 0.29474\,s^5 - 0.416708\,s^4 - 0.143452\,s^3 \\ -\,0.0201614\,s^2 - 0.0012663\,s - 0.0000295384 \end{matrix}\right)e^{-6.79s}}{\left(\begin{matrix} 1.03s^6 + 3s^5 + 1.98\,s^4 + 0.471s^3 + 0.05s^2 \\ +\,0.00235s + 0.0000401624 \end{matrix}\right)(\tau_2 s+1)} \qquad (51)$$

With tuning parameters set as $\boldsymbol{\tau_1 = 31, \tau_2 = 31}$, the two controllers are reduced using moment matching to

$$\boldsymbol{C_{r\_perfy1}} = \begin{bmatrix} \frac{(9.15462\,s^2 - 8.23268\,s - 0.66757)e^{-3.13s}}{728.07\,s^2 + 54.5297\,s + 1} & \frac{(138.282\,s^2 + 38.145\,s + 1.22579)e^{-7s}}{1023.96\,s^2 + 63.2592\,s + 1} \\ \frac{(273.169\,s^2 + 38.5057\,s + 1.11997)e^{-2.09s}}{632.057\,s^2 + 51.0229\,s + 1} & \frac{(-149.452\,s^2 - 15.97\,s - 0.73548)e^{-5s}}{365.795\,s^2 + 43.6244\,s + 1} \end{bmatrix} \qquad (52)$$

$$\boldsymbol{C_{r\_perfy2}} = \begin{bmatrix} \frac{(-126.014\,s^2 - 15.031\,s - 0.667571)e^{-5s}}{547.585\,s^2 + 49.1456\,s + 1} & \frac{(3854.23\,s^2 + 404.806\,s + 1.226)e^{-2.83s}}{10426.8\,s^2 + 352.968\,s + 1} \\ \frac{(26.6341\,s^2 + 16.9705\,s + 1.11997)e^{-8s}}{773.562\,s^2 + 55.8324\,s + 1} & \frac{(9.1582\,s^2 - 5.93531\,s - 0.7355)e^{-6.79s}}{731.586\,s^2 + 54.6372\,s + 1} \end{bmatrix} \qquad (53)$$

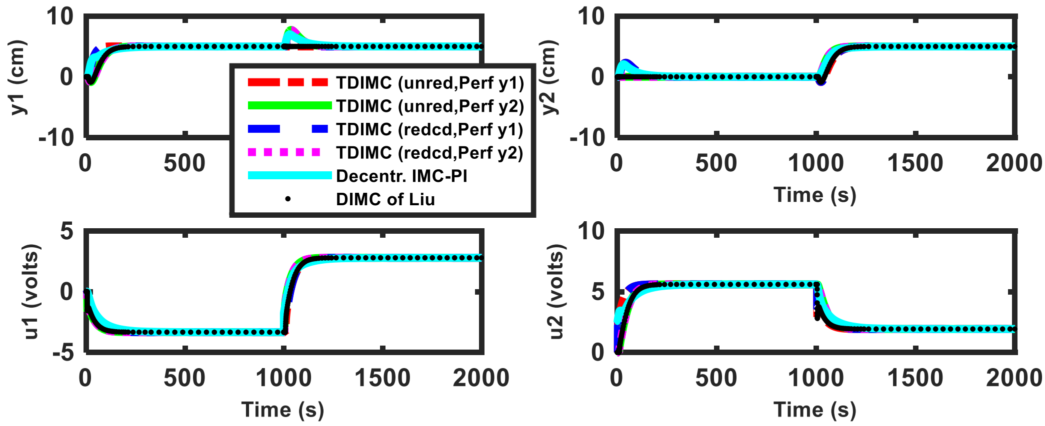

Figure 2: Plant Output and Input Responses of Triangular DIMC, Dynamic DIMC and Decentralized IMC-PI Schemes on NMP QTPwDTs. Step Commands are of Sizes 5cm each, introduced at 0s and 1000s respectively

Table 1: Comparison of Performance Indices, on One Hand, and Advantages and Disadvantages, on the Other Hand, of the Triangular DIMC Methods with Dynamic DIMC and Decentralized IMC-PI Methods

Controller	IAE	TV	μ_{RS}	μ_{RP}	Advantages	Disadvantages
Triangular DIMC (Unreduced, Perfect y_1)	809.8	10.95	0.1999	0.9035	Most important output(s) has/have near-perfect response.	One output (least important) has inverse response and therefore has a constraint on bandwidth due to RHP zero, high-order controllers
Triangular DIMC (Unreduced, Perfect y_2)	918.2	11.36	0.1994	0.9615	Most important output(s) has/have perfect response.	One output (least important) has inverse response and therefore has a constraint on bandwidth due to RHP zero, high-order controllers
Dynamic DIMC of Liu	893	12.60	0.1025	0.8190	Outputs are controlled separately, little or no control-loop interactions	Both outputs have inverse responses and therefore have bandwidth constraints due to RHP zero
Triangular DIMC (Reduced, Perfect y_1)	812.9	14.95	0.1998	0.9060	Has advantages of TDIMC (perf. y_1) but with simpler controllers	Same as TDIMC (perfect y_1)
Triangular DIMC (Reduced, Perfect y_2)	919.0	17.08	0.1999	0.9612	Has advantages of TDIMC (perf. y_2) but with simpler controllers	Same as TDIMC (perfect y_2)
Decentralized IMC-PI	971.8	18.56	0.0285	0.7553	Simplest controllers of all six, possibility of little or no inverse response due to interaction zero.	Control-loop interactions significant

For comparison, the analytically-derived DIMC scheme was designed for the system using the method of Liu and co-workers (2006). Also, a decentralized IMC-PI scheme was also designed for the system using the IMC-PI tuning rules of Chien and Fruehauf (1990). Because of space economy, the details of the designs are not presented. Figure 2 shows the comparison of the plots of the manipulated and controlled variables for the two unreduced triangular DIMC designs, the two reduced triangular DIMC designs, the dynamic DIMC design of Liu and co-workers, and the decentralized IMC-PI design on the linear NMP plant. In each implementation, $\boldsymbol{\tau_1 = 31, \tau_2 = 31}$. Table 1 shows a comparison of the performance indices (output IAE, input TV, $\boldsymbol{\mu_{RS}}$ and $\boldsymbol{\mu_{RP}}$) and presentation of advantages and disadvantages of the decentralized, dynamic decoupling IMC and triangular decoupling IMC implementations. As seen in the plots, the unreduced triangular decoupling IMC methods successfully transfer inverse response behaviour and interactions to the least desired output while still achieving output IAE and input TV values that compare favourably with those obtained using the dynamic DIMC technique of Liu and co-workers (2006).

The Triangular DIMC method, as explained in Table 1, has the advantage of absence of bandwidth restrictions imposed by NMP behaviour on the system for all but one of the outputs of the system, an advantage that is valuable in multivariable situations where some outputs are preferred to others (for example, the Sugar Mill situation of Goodwin *et al.* (2000)). Also, this advantage becomes more pronounced as the number of outputs of the system increases. The output IAE value of the unreduced controllers achieving perfect $\boldsymbol{y_1}$ is lower than that of dynamic DIMC of Liu and co-workers, while the input TV values for both unreduced controllers achieving triangular decoupling are lower than those of Liu and co-workers. The reduced triangular DIMC controllers have marginally worse values of output IAE and input TV than the unreduced ones because of the marginal imperfections occasioned by the reductions. The decentralized IMC-PI controllers performed marginally below the other controllers because of the interactions that are not catered for, but has the simplest structure of all the 6 control systems. All designs satisfied the conditions for the existence of robust stability and robust performance.

8. Conclusions

In this study, a modification to the traditional dynamic decoupling internal model control scheme has been proposed to achieve triangular decoupling. The study formulated the desired closed-loop transfer function matrix and the corresponding centralized IMC controller that both achieve the shifting of interaction and inverse-response behaviours to each of the two outputs, while ensuring that the other output is without interaction behaviour and without inverse response behaviour. The formulation is implemented on the NMP Quadruple-Tank Process of Shneidermann and Palmor (2010) and shown to achieve the set objectives, as shown in Figure 2.

As shown in Table 1, triangular DIMC is capable of yielding better output IAE and input TV values than the dynamic DIMC implementations of Liu and co-workers for square stable TITO systems with delays and RHP zeros, while also ensuring that bandwidth limitations due to NMP behaviour are restricted to a single output as opposed to the dynamic DIMC case where bandwidth limitations due to NMP behaviour affect both outputs. The extensions of the techniques of Frank (1974), on one hand, and Inner-Outer Factorization of Morari and Zafiriou (1989) to square multivariable systems with delays promise to achieve more optimal outcomes than the triangular decoupling IMC schemes in this paper and are therefore worth pursuing.

References

Chien, I-L, and Fruehauf, P.S. (1990), “Consider IMC Tuning to Improve Controller Performance,” *Chem. Eng. Progress*, **86** (10), 33.

Descusse, J., and Lizarzaburu, R. (1979), "Triangular Decoupling and Pole Placement in Linear Multivariable Systems: A Direct Algebraic Approach," *Int. Journal of Control*, **30** (1), 139-152.

Economou, C.G. and Morari, M. (1986), "Internal Model Control. 6. Multiloop Design" *Ind. Eng. Chem. Process Des. Dev.*, **25**, 411–419.

Economou, C.G., Morari, M. and Palsson, B.O. (1986), "Internal Model Control. 5. Extension to Nonlinear Systems," *Ind. Eng. Chem. Process Des. Dev.*, **25** (2), 403–411.

Frank, P.M. (1974), *Entwurf von Regelkreisen mit Vorgeschrieben Verhalten*, G. Braun, Karlsruhe, Germany.

Garcia, C.E., and Morari, M. (1982), "Internal Model Control. 1. A Unifying Review and Some New Results," *Ind. Eng. Chem. Process Des. Dev.*, **21**, 308-323.

Garcia, C.E., and Morari, M. (1985), "Internal Model Control. 2. Design Procedure for Multivariable Systems," *Ind. Eng. Chem. Process Des. Dev.*, **24**, 472-484.

Garrido, J., Vazquez, F. and Morilla, F. (2014), "Inverted decoupling internal model control for square stable multivariable time delay systems," *Journal of Process Control*, **24**, 1710-1719.

Goodwin, G.C., Graebe, S.F., and Salgado, M.E. (2000), *Control System Design*, Prentice-Hall, Englewood Cliffs, New-Jersey, United States of America.

Holt, B.R. and Morari, M. (1985), "Design of Resilient Processing Plants—VI. The Effect of Right-Half-Plane Zeros on Dynamic Resilience," *Chemical Engineering Science*, **40** (1), 59-74.

Koumboulis, F.N., and Kouvakas, N.D. (2018), "Delayless Controllers for Triangular Decoupling with Simultaneous Disturbance Rejection of General Neutral Time-Delay Systems," *Proceedings of the 26th IEEE Mediterranean Conference on Control and Automation*, June 19-22, 2018, Zadar, Croatia, pp. 741-746.

Koumboulis, F.N. and Panagiotakis, G.E. (2008), "Transfer Matrix Approach to the Triangular Decoupling of General Neural Multi-Delay Systems," *Proceedings of the 17th World Congress of The International Federation of Automatic Control*, July 6-11, 2008, Seoul, South Korea.

Koumboulis, F.N., and Skarpetis, M.G. (2000), "Robust Triangular Decoupling via Output Feedback," *Journal of the Franklin Institute*, **337**, 11-20.

Li, M., Jia, Y. and Liu, H. (2017), "Static State Feedback Triangular Block Decoupling for Arbitrary Systems: A State Space Method," *Int. Journal of Control*, **90** (7), 1428-1436.

Liu, T., Zhang, W., Gu, D. (2006), “Analytical Design of Decoupling Internal Model Control (IMC) Scheme for Two-Input-Two-Output (TITO) Processes with Time Delays,” *Ind. Eng. Chem. Res.*, **45**, 3149-3160.

Morari, M. and Zafiriou, E. (1989), *Robust Process Control*. Prentice Hall, Englewood Cliffs, New Jersey, United States of America.

Morse, A.S. and Wonham, W.M. (1970), "Triangular Decoupling of Linear Multivariable Systems", *IEEE Trans. on Automatic Control*, Short Paper, 447-449.

Nijmeijer, H. (1984), "The Triangular Decoupling Problem for Nonlinear Control Systems," *Nonlinear Analysis. Theory, Methods and Applications*, **8** (3), 273-279.

Nguyen, H.T., and Su, S.W. (2009), "Conditions for Triangular Decoupling Control," *Int. Journal of Control*, **82** (9), 1575-1581.

Shen, D., and Wei, M. (2015), "The Pole Assignment for the Regular Triangular Decoupling Problem," *Automatica*, **53**, 208-215.

Shneidermann, D. and Palmor, Z.J. (2010), “Properties and Control of the Quadruple-Tank Process with Multivariable Dead-Times,” *Journal of Process Control*, **20**, 18-28.

Skogestad, S. and Postlethwaite, I. (2005), *Multivariable Feedback Control: Analysis and Design* (2nd ed.), John Wiley & Sons Inc., Chichester, United Kingdom.

Wang, Q.G., Zhang, Y. and Chiu, M.S. (2002); “Decoupling Internal Model Control for Multivariable Systems with Multiple Time Delays,” *Chemical Engineering Science*, **57**, 115-124.

Wang, S.W. (2007), "Relationship between Triangular Decoupling and Invertibility of Linear Multivariate Systems," *Int. Journal of Control*, **15** (2), 395-399.